Metatranscriptomic approach for microbiome characterization and host gene expression evaluation for “Hoja de malvón” disease in *Vitis vinifera* cv. Malbec

Marcos Paolinelli (paolinellimarc@gmail.com)
CONICET Mendoza https://orcid.org/0000-0003-0098-0646
Georgina Escoriaza
Instituto Nacional de Tecnologia Agropecuaria
Cecilia Cesari
Instituto Nacional de Tecnologia Agropecuaria
Sandra Garcia-Lampasona
Instituto Nacional de Tecnologia Agropecuaria
Rufina Hernandez-Martinez
Centro de Investigacion Cientifica y de Educacion Superior de Ensenada

Research

Keywords: RNAseq; GTD; metatranscriptomics; Vitis vinifera, high throughput sequencing

Posted Date: April 21st, 2020

DOI: https://doi.org/10.21203/rs.3.rs-23526/v1

Abstract

Background: Grapevine Trunk Diseases (GTD) threat worldwide wine and table grape production, mainly reducing grape yields and in advanced stages causing the death of diseased vines. A particular GTD of enormous concern in Argentinean vitiviniculture is the complex etiology disease locally known as "Hoja de malvón" (HDM). At least four different fungi are involved in the disease, which complicates the diagnostic and the design of strategies for vineyard management. Similar to Esca grape disease, factors that make this disease difficult to control are the presence of pathogens that not always correlates with disease symptoms or physiological changes in the host. Also the abiotic stress on grapevine seems to favors the disease process. Based on this background, it is essential to have molecular tools that allow for simultaneous explorations of the host immunity status and the microbiome composition.

Results: A metatranscriptomic approach was followed and different strategies for microbiome characterization, throughmolecular marker reconstruction or unique kmer counts, were evaluated. Malbec microbiome was mainly represented for Dothideomycetes and Actinobacteria. Higher Basidiomycota/Ascomycota ratio was found in symptomatic (SYM) than in asymptomatic (ASYM) plants, with the Basidiomycota *Arrambaria destruens* found in higher levels in SYM plants. Besides, from mRNA-derived reads, the host functional status and main microbial functions based on gene expression were evaluated. Stress-tolerance mechanisms were activated on ASYM plants, being spermidine synthesis one of the most important, while from the microbiome side, prokaryotic tricarboxylic acid pathways were the primary differential function in SYM plants.

Conclusions: This is a pioneering work for the characterization of multi-kingdom endophytic microbiome in woody tissues of grapevine cv. Malbec. Several microorganisms with negative interaction with GTD pathogens were identified and can be further explored as biological control agents for HDM disease. The integral analysis employed suggests that measuring Basidiomycota/Ascomycota ratio and spermidine-associated gene expression would help to monitor the sanitary status of grapevine and the propensity to develop HDM disease. This study provides a departure point for a better comprehension of HDM disease that can be used as a roadmap for further development of curative practices of GTD.

Background

Grapevine Trunk Disease (GTD) is one of the main concerns for vitiviniculture worldwide. GTD is a general term that refers to all the diseases caused by fungi that affect grapevine wood. Although sometimes pathogens are found mixed on symptomatic tissues, based on characteristic symptoms and the causal agents involved, specific disease names were assigned. Esca grape disease is caused by *Phaeomoniella chlamydospora*, *Phaeoacremonium* spp., and *Fomitiporella* spp. Esca is one of the most important GTD; its etiology still is under discussion. The most accepted hypothesis is that young vines become infected with the pioneer fungi *P. chlamydospora* and *Phaeoacremonium* spp. and later with Basidiomycete fungi from the genera *Inocutis*, *Inonotus*, *Stereum*, *Phellinus*, *Fomitiporia*, and *Fomitiporella* [1]. The causal agents of Botryosphaeria dieback are Botryosphaeriaceae fungi, from the genera *Botryosphaeria, Diplodia, Dothiorella, Lasiodiplodia, Neofussicoccum, Neoscytalidium, Phaeobotryosphaeria*, and *Spencermartinsia*. *Eutypa lata* causes Eutypa dieback, *Phomopsis* spp. causes Phomopsis dieback, and *Cylindrocarpon* spp. and *Campylocarpon* are the causal agents of black foot disease [1]. Grapevine plants have died in the vineyard because of GTD since ancient times, but the diseases used to have low incidence; however, in the last 20–30 years, they became a serious problem worldwide, with frequencies reaching up to 80% of vines in a vineyard [1]. Despite intense research, still, there are not therapeutic practices for GTD, mainly because of the complex etiology associated with them. The increase in GTD worldwide is attributed to changes in cultural practices (i.e. conducting systems that require intense pruning), climate changes favorable for pathogen fitness, higher dissemination of pathogens due to international transport of propagation material, and absence of free-pathogen plant stocks in nurseries [1]. The risk of spread is associated with the capacity of those pathogens to have a long asymptomatic phase, which makes it more difficult for the early detection and the elimination of infected material before plantation. Nowadays, the recommended preventative practices are minimization of wounds during pruning, wound protection, production of pathogen-free propagation material, and periodic monitoring of the pathogen inoculum in the field through molecular methods [1].

Argentina's vitiviniculture has a big concern because of GTD, mainly with the Esca-like disease known as "Hoja de malvón" (HDM) [2]. The disease begins in one of the arms of the plant, affecting branches, leaves, and clusters. Leaves have a smaller size, become chlorotic, and with the inscribed edges curled down, taking the appearance of a "geranium" leaf, from which the disease takes the name. The shoots have less growth and shorter internodes than those in healthy plants. The clusters are smaller, lax, and without uniform grains. In the transverse section of the trunk, necrosis of different colorations and consistencies are observed that indicate the progression of the disease [2]. In the trunk of some plants, the presence of light brown colored symptoms is observed, corresponding to basidiocarps of the fungus *Arambarria destruens* (formerly *Inocutis jamaicensis*) [3]. In Chile, similar symptoms are observed for a disease named "Enrollamiento clorótico de la vid" [4]. Around the world in Esca disease, *Phaeoacremonium* spp. and *P. chlamydospora* are always isolated and are associated with different Basidiomycota-Hymenomycete fungi. In Europe and the Mediterranean grape-growing regions, *Fomitiporia mediterranea* is the prevalent species; in Chile *Fomitiporella vitis* and, in Australia, *Fomitiporia australiensis* [5]. In Argentina, the Basidiomycota was identified as *Inonotus sensu lato* (*Inocutis* Fiasson & Niemelä) [3], later reclassified as *Inocutis jamaicensis* [6] and recently, recognized as a new species named *Arambarria destruens* [7]. *P. aleophilum* and *P. chlamydospora* are frequently isolated from symptomatic tissues, but in lower frequency than the Hymenomycete *A. destruens*. HDM is commonly found in Argentinean vineyards in more than 20 years old plants, which correspond to 46.8% of the total vineyards of the country [8]. In Argentina, old vineyards are maintained because of the wine quality obtained from the plants and for the economic limitations to replant vineyards. This particularity obliges to reinforce disease prevention through periodic monitoring of the vineyard, reducing the opportunity to get infected plants with GTD.

The monitoring of GTD pathogens on vines is mainly done using conventional cultural isolations coupled to morphological characterization. Few molecular techniques for pathogen monitoring have been developed [9–11], but little has been done regarding HDM disease. Molecular tools are needed to understand the importance of each pathogen involved in HDM disease that correlates with the presence of symptoms and to understand which physiological change makes grapevine more susceptible. A non-destructive and easy to adopt technique will facilitate extensive analyses of the pathogens present in vineyards. Molecular techniques based on high throughput sequencing (HTS) are more adaptable than conventional cultural-based techniques to reach such aim.

Different techniques have been used to characterize the microbiome associated with *Vitis vinifera*. First, cultural isolation and molecular characterization through Sanger sequencing [12–13], Later, culture-independent methods, including automated ribosomal intergenic spacer analysis (ARISA), denaturing gradient gel electrophoresis (DGGE), and single-strand conformation polymorphism (SSCP) [14]. Recently, the studies of the grapevine microbiome increased markedly using amplicon sequencing [15–20]. Previous works performed to understand the relationship between microbiome and GTD have been done [21–27], but only Morales-Cruz et al. (2018) explored the grapevine microbiome using metagenome and metatranscriptome approaches [11]. The current accessibility to HTS, their higher sensibility, and the development of efficient computational algorithms increase the possibility to explore the uncultivable and less abundant microorganisms.

The metatranscriptomics approach allows for the direct inspection of the whole sanitary status of a plant because of the simultaneous detection of several pathogens like viruses, bacteria, fungi, and archaea in a kingdom-independent manner. Also, it is possible to characterize the metabolically active microorganisms, avoiding the dead ones considered in a metagenomics approach. This approach could help to understand the interaction established among the microorganisms with their host, from a functional point of view.

Based on previous reports on GTD, abiotic stress predispose plants to fungal pathogen colonization, evidencing the importance of having a simultaneous exploration of the pathogen and the status of the host. Although several endophytic microbiome characterizations of different grapevine cultivars have been done worldwide on the main wine-producing regions [14], to the best of our knowledge, there is no previous exploration of the microbiome in *Vitis vinifera* cv. Malbec cultivated in the Mendoza region. Thus, this work aimed to identify differences in terms of microorganisms and plant gene expression that could help to identify molecular markers for monitoring and the early detection of HDM in vineyards. For that, a simultaneous exploration of both microbiome and host gene expression in symptomatic and asymptomatic plants of *Vitis vinifera* cv. Malbec was performed.

Results

Grapevine endophytic microbial composition determined through culture isolation and morphological characteristics

Based on the morphological characteristics observed in the isolated microorganisms, seven filamentous fungi were characterized to the genus level, yeasts where distinguished based on morphology, and bacteria were only distinguished at the Domain taxonomic level (TableS1.xlsx). The main fungal genus isolated was *Alternaria* sp. (ranging from 0.35 to 0.61 relative abundance) followed by *Penicillium* sp. (from 0.24 to 0.44 relative abundance) and yeasts in minor frequency (from 0.08 to 0.3). *Cladosporium* sp. (from 0.04 to 0.12 relative abundance), *Epicoccum* sp. (from 0.04 to 0.08 relative abundance), and *Trichoderma* sp. (0.04 relative abundance only in sample c23). Also, two well-known pathogens in HDM disease were identified: *Arambarria sp*. (from 0.06 to 0.16) and *Phaeoacremonium* sp. (0.032 relative abundance only in sample m11). *Arambarria* sp. was isolated in the three SYM plants and one ASYM plant (sample c22). This sample was not used in further comparative analyses because careful examination of transversally cut branches showed evidence of white-rot symptoms, which are typically observed in grapevine with HDM.

Grapevine Endophytic Microbial Composition Determined Through Metatranscriptomics

The RNAseq rendered an average of 18,567,374 paired reads (37,134,748 unpaired) having an average length of 100 bp with a GC% content of 50.53 and 92.9% reads above the Q30 Phred quality (TableS2.xlsx) per sample. After quality revision and trimming, an average of 18,206,455 high quality paired reads remained. The reads that belong to the grapevine host were separated from those coming from microorganisms through mapping on *V. vinifera* cv. Pinot Noir PN40024 genome. An average of 55.4% reads was uniquely mapped on the grapevine genome and used for gene expression analysis. The unmapped reads (average of 42.7%; TableS2.xlsx) were used for microbial identification and quantification through a phylogenetic marker reconstruction approach or identifying and counting unique kmers.

Microbiome Prokaryotic Composition Determined Through Phylogenetic Marker Reconstruction

The reconstruction of 16S phylogenetic marker through MATAM software allow us to determine that Bacteria were the most abundant prokaryotic domain representing 5–9%, while Archaea only represented 0-0.3% from the entire community and was mainly enriched in ASYM plants (FigureS1.html). The genus of Archaea found in SYM plant was *Nitrososphaera sp*. (0.03%) identified only in m26 SYM plant, while in ASYM plants besides *Nitrososphaera* sp. (0.02–0.03%), *Halococcus* sp. (0.03–0.3%) and *Halalkalicoccus* sp. (0.03%) were present (FigureS1.html). On other hand, under Bacteria domain, Actinobacteria (2–4%), Bacteroidetes (1–3%), and Proteobacteria (1–2%) were dominant at Phylum taxonomic level (Fig. 1 and FigureS1.html). At the genus level *Segetibacter* sp. (0.8-1%), *Pseudonocardia* sp. (0.3-1%), *Modestobacter* sp. (0.5–0.8%), *Hymenobacter* sp. (0.2–0.9%), *Sphingomas* sp. (0.3–

0.6%), and *Massilia* sp. (0.3–0.7%) were present in high proportions in all the samples; while *Singulisphaera* sp. was more represented in ASYM vines (0.3–0.6% in ASYM and 0.01–0.1% in SYM) (Fig. 1 and FigureS1.html)

Microbiome Eukaryotic Composition Determined Through Phylogenetic Marker Reconstruction

LSU marker reconstruction and SILVA-LSU DB were used as a reference to characterize eukaryotic microbiomethrough MATAM software. Metazoa represented 2–14% of all the reads, while Fungi represented 6–19% (FigureS2.html). The rest of the classified taxa corresponded to Oomycetes (1–2%), Amoebozoa (0-0.7%), and Alveolata (0-0.2%, FigureS2.html).The ribosomal RNA SILVA-LSU DB was not adequate for fungal classification in low taxonomic levels (genus and species) because most of the taxonomic names assigned to the sequences deposited there are out of date, and most of the associated GTD pathogens are absent (which is the focus of this research). Therefore, fungal community characterization shown here is based on MATAM classification using Warcup-RDP-ITS, an alternative updated reference for fungi [28]. Ascomycota was almost the unique represented phylum (97–99% of all the identified fungi. Figure 1 and FigureS3.html). Basidiomycota represented only around 0-0.3% in ASYM plants and 0.4–0.9% in SYM plants (Fig. 1 and Figure S3.html). From the Ascomycota, the Dothideomycetes were the most abundant (54–72% of all the identified fungi) at the class taxonomic level, followed by Sordariomycetes (7–19%), Eurotiomycetes (7–15%), Leotiomycetes (6–10%), and Pezizomycetes (2–6%) (FigureS3.html). The most abundant class under Basidiomycota phylum was Agaricomycetes (ASYM: 0-0.2% and SYM: 0.3–0.9%, FigureS3.html). At the taxonomic order level under the Dothideomycetes class, Pleosporales and Capnodiales were the most abundant, with 47–65% and 3–9% of Fungi, respectively. Botryosphaeriales were low represented (0.03% of Fungi) being *Camarosporium brabeji* (only in m16) and *Microdiplodia miyakei* the unique identified species (FigureS3.html).

The most represented genera on the fungal community were *Alternaria* sp. (23–43% of Fungi), *Massarina* sp. (15–32%), and *Exophiala* sp. (7–15%) (Fig. 1 and FigureS3.html). Despite showing high variability, *Pestalotiopsis* sp. was more represented in ASYM (0.5–10%) than SYM (0.8-1%, Fig. 1 and FigureS3.html).

Microbiome Based On Counts Of Unique Identified K-mers

KrakenUniq software subdivide the HTS reads in kmers and make an indexation for identification of the unique kmers that are used to taxonomic assignment based on NCBI 'NT' DB. Bacteria identified through this strategy represented 7–9% from total sequences (FigureS4.html and TableS3.xlsx), while Archaea ranged from 0.3 to 0.4% and eukaryotic members represented 9–11%, being mostly represented by Fungi (6–7% of all the microorganisms identified as Eukaryota). Oomycetes were also identified in low proportions (1% of Eukaryota) (FigureS4.html and TableS3.xlsx).

Microbiome Bacterial Composition Based On Unique Kmer Counts

The primary represented bacterial Phylum was Actinobacteria (20–21%; Fig. 2A, FigureS4.html, and TableS3.xlsx) followed by Alphaproteobacteria (14–15%), Gammaproteobacteria (16–17%), Betaproteobacteria (7%), Bacilli (6%) and Clostridia (4%) (Fig. 2A, FigureS4.html, and TableS3.xlsx). Compared with relative abundance determined through MATAM, the unique kmer counts coincided with the determination of Actinobacteria as the most abundant Phylum. On the other hand, Bacteroidetes were the second most abundant based on MATAM, but based on KrakenUniq output, they were recognized as relatively abundant (7%) but bellow of Firmicutes (11%) and Proteobacteria (42–43%). In MATAM output, Firmicutes were not recognized at all.

At the genus level, the differences with MATAM were even more evident; for instance, the relative abundance of *Segetibacter* sp. was around 0.03–0.04%, according to KrakenUniq, quite different from 10–18% obtained with MATAM. Similar differences were found for *Pseudonocardia* sp. (6–13% in MATAM vs 0.4–0.5% in KrakenUniq), *Modestobacter* sp. (7–10% in MATAM vs 0.08-1% in KrakenUniq), *Hymenobacter* sp. (7–10% in MATAM vs 0.2–0.3% in KrakenUniq), *Sphingomas* sp. (4–8% in MATAM vs 0.9% in KrakenUniq) and *Massilia* sp. (4–9% in MATAM vs 0.07–0.1% in KrakenUniq)

Microbiome Fungal Composition Based On Unique K-mers Counts

From fungal classified sequences, Ascomycota represented 67–74% and Basidiomycota 19–25% (FigureS4.html and TableS3.xlsx). Also, at very low percentages (< 3%) were identified other Phyla: Mucoromycota, Zoopagomyota, Chytridiomycota, Blastocladyomycota, Cryptomycota, and Entorrhizomycota. At the taxonomic class level, Dothydeomycetes represented 22% of the fungal community, followed by Sordariomycetes 17–18%, Eurotiomycetes 8%, Leotiomycetes 4–5%, Pezizomycetes 2%, Agaricomycetes (10–16%), Lecanoromycetes (8–9%) and Saccharomycetes (5–6%) (Fig. 2 and Figure S4.html).At the taxonomic order level, Pleosporales were the most represented (46–63%); followed by Chaetothyriales (2.8–4.6%), Eurotiales (2.4-4%), Dothideales (1.1–4.1%), Capnodiales (1.8–2.8%); Glomerellales (0.7–1.4%). Botryosphaeriales were low represented (< 0.01% in all the samples), and Melanosporales were found in very low proportion (< 0.001%).

At the taxonomic family level, the most represented were Pleosporaceae (22–41%); *Leptosphaeriaceae* (4.4–9.4%), *Phaeosphaeriaceae* (4.8–7.8%), *Didymellaceae* (ASYM: 3.6–5.2%; SYM: 1.4–1.7%), *Didymosphaeriaceae* (0.9–2.9%), *Mycosphaerellaceae* (1.12–1.96%), *Saccotheciaceae* (0.9–1.8%), *Nectriaceae* (0.8–1.1%), *Aspergillaceae* (1.9–3.3%), *Herpotrichiellaceae* (2.4–3.3%)(Fig. 2, FigureS4.html and TableS3.xlsx). *Lophiostomataceae* was one

of the most abundant based on MATAM (15–32% of Fungi) but was low represented (0.3–0.4%) using KrakenUniq. At the genus level, only the species that quite supported the MATAM-based analysis were used for classification method comparison with the KrakenUniq output (Table I).

Table I. Fungal Species classification and relative abundance according to the method used: MATAM vs. KrakenUniq (Values graphically represented in FigureS3.html and FigureS4.html)

Fungal Genus Identified	MATAM-based percentage respect to the total abundance of Fungi	KrakenUniq-based percentage respect to the total abundance of Fungi
Exophiala sp.	7–15	0.4–0.5
Morchella sp.	3–5	0.05–0.09
Cryptococcus sp.	0–0.9	0.3 in all samples
Rhodotorula sp.	0-0.05	0.2 in all samples
Leveillula sp.	6–10	0-0.05
Cladosporium sp.	3–8	0.4–0.5
Davidiella sp.	3–9	0.01
Fusarium sp.	4–7	1
Harzia sp.	0-0.1	0.2
Nigrospora sp.	2–3	0.06–0.09
Pestalotiopsis	0.5–10	0.1–0.2
Morinia sp.	0-0.2	0.1–0.2
Paraconiothyrium sp.	0-0.07	0.4–0.6
Periconia sp. (*Massarina* sp. in MATAM)	15–32	0.07–0.1
Coniothyrium sp.	0-0.04	Not found
Alternaria sp.	23–43	1

The comparison of methods used for microbiome determination showed significant differences. For KrakenUniq, in general, the lower percentage for microbiome members was accompanied by higher diversity in terms of richness. However, there are some exceptions, i.e. *Paraconiothyrium* sp. and *Harzia* sp. that were quantified in higher relative abundance in KrakenUniq output than in MATAM output (Table I).

Interaction Between Microorganisms Based On The Correlation Matrix

Without taking into consideration the origin of the sample, a matrix of correlations was done for the fungal community to identify putative biological control agents (BCAs) interacting negatively with GTD pathogens. Focusing on the pathogens *A. destruens* and *P. minimum*, the primary negatively interacting fungi were found in the order Pleosporales, which includes *Alternaria alternata*, *Alternaria solani, Parastagonospora nodorum* and *Didymella pinodes* (Fig. 3). Also, it was clear that there are mainly inverse correlations between Basidiomycota and Ascomycota fungi (Fig. 3 and FigureS5.pdf).

Microorganism Differentially Abundant In Sym Vs. Asym Comparison

The multidimensional scaling (MDS) analysis of unique kmers counts, for each identified taxon derived from KrakenUniq output, indicate that c23 and c25 had a similar microbial composition. The similarity between both samples was enough higher than the obtained with the samples of SYM plants (FigureS6.pdf). At the same time, c22 was different from the others ASYM samples, which agrees with the isolation of *A. destruens* on that sample. On the other hand, from SYM plants, m11 and m26 despite having a sparse microbial composition were more similar between them than sample m16, which shows a clear enrichment in the Basidiomycota phylum (Fig. 2A). The symptoms from m16 sampled plants were more pronounced, as a branch was severely affected than those obtained from m11 and m26, indicating that the increase in Basidiomycota corresponds to the decay of vine tissues, typical behavior of fungi involved in white rot. This fact was taken into consideration for further statistical analyses, and only the unique kmers counts obtained from c23 + c25 in ASYM plants and m11 + m26 in SYM were used. The comparison showed that three genera of Archaea have significant relative abundance differences (FDR < 0.15). *Halococcus* sp., *Haloquadratum* sp., and *Halalkalicoccus* sp. presented higher relative abundance in ASYM plants (Fig. 4 and TableS4.xlsx). In contrast, *A. destruens* showed a higher relative abundance in SYM plants (Fig. 4 and TableS4.xlsx). Several other GTD pathogens were identified through KrakenUniq, Botryosphaeriaceae (*Neofusicoccum parvum* and *Diplodia corticola*), *P. minimum*, and *E. lata*, but they had similar relative abundance in both SYM and ASYM plants.

The relative abundance of Actinobacteria was higher in SYM than in ASYM plants (FDR < 0.15, Fig. 4 and TableS4.xlsx). It was remarkable that ten species of Basidiomycetes were highly abundant in SYM compared to ASYM plants (FDR < 0.15, Fig. 4, TableS4.xlsx). Besides *A. destruens*, the other nine Basidiomycota taxa that were identified as significantly different were *Pterula* affinis *epiphylloides*, *Pterula sp*. BZ3484, *Junghuhnia nitida*, *Rhizoctonia solani*, *Suillus sinuspaulianus*, *Phellinus laevigatus*, *Hericium coralloides*, *Thelephora ganbajun*, and *Pleurotus citrinopileatus*.

Microbial Functional Pathways In Sym Vs. Asym Grapevines Comparison

Functional pathways enrichment analyses from the multi-kingdom microbiome independently of the microorganisms that codes for the function, identified Tricarboxylic Acid (TCA)-cycles pathways (PWY-6969, P105-PWY and TCA-cycle I from prokaryotes) as the most significant functions in SYM vs. ASYM plants (p-value < 0.05 in ANOVA Tukey-Kramer's test) (Fig. 5 and TableS5.xlsx). Also, the TCA-glyoxylate bypass pathway was induced differentially in SYM plants. These results indicate that the induction of the central TCA cycle is important for the microorganisms hosted by SYM plants.

Grapevine Gene Expression And Functional Enrichment Analysis

Using counts of reads mapped in the Pinot Noir PN40024 grapevine reference genome, the differential gene expression was calculated. Fifty-seven up-regulated genes, and 159 down-regulated genes were identified (Using a threshold of FDR < 0.05). The grapevine Gene Ontology (GO) term enrichment analysis in SYM vs. ASYM plants, GO:0008295 'spermidine biosynthesis process' was enriched among downregulated genes when considering FDR < 0.05 threshold, and 34 GO terms were enriched when considering a p-value < 0.005 as a threshold (Fig. 6 and TableS6.xlsx). The primary function in SYM plants was the repression of genes that codify for proteins with nuclear localization (GO:0005634), mainly involved in the regulation of transcription (GO:0006355). The spermidine (GO:0008295), spermine (GO:0006597), and S-adenosylmethioninamine (GO:0006557) biosynthetic processes; and the arginine decarboxylase (GO:0008792) and adenosylmethionine decarboxylase (GO:0004014) activities were repressed. All those processes are involved in polyamine synthesis pathways, indicating that polyamines are underexpressed in SYM plants. The activities of cellular response to heat (GO:0034605), trehalose metabolism in response to stress (GO:0070413), and trehalose-phosphatase activity (GO:0004805) were also repressed.

Discussion

According to the results, a considerable microbial diversity constitutes the grapevine cv. Malbec endophyte population. The best identification was done when using the unique kmer for microbial classification with 24,851 putative identified species (549 with relative abundance > 0.0001). Forty-one point nine percent (10,410 species) belong to the fungal kingdom, 37.8% (9,391 species) to Bacteria and 1.4% (345 species) to Archaea Domains. The NT DB contains 1,355,495 species [29], the number of species here identified corresponds just to 1.8% of the total available species in NT DB, revealing the discriminating power of KrakenUniq classification process. When using the reconstruction of 16S and ITS markers for classification, a much lower number was found with 40 fungal species, 26 bacterial genera, and only one Archaea genus. The results obtained with each method were contrasting and extreme because, in previous works, around a hundred to thousand species where found in the endophytic community of *V. vinifera* vascular tissue [14]. Based on the threshold of relative abundance higher than 0.0001, the species identified through the unique kmer strategy were 549, which is more similar to the expected results with a lower probability to have false-positive results. The 67 genera identified through MATAM strategy seems to underestimate 'the real' diversity. An explanation for obtaining a higher number of designated microorganisms and even at a deeper taxonomy level could be that KrakenUniq uses the most resolute molecule in terms of uniqueness from several options, while MATAM only considers one molecular marker.

The approach used here, based on the sequencing of ribodepleted RNA, was chosen to enrich the target host mRNA molecules and the rRNA from a microbial community. To the best of our knowledge, this is the first time this strategy is used for the study of the GTDs-grapevine pathosystem. One of the main advantages over DNA sequencing-based techniques, is the identification of only living microorganisms or the functional ones, due to the short lifetime of the RNA molecule. Another advantage is that several molecular markers can be used to explore the community from the same sequencing run. A disadvantage is that a considerable sequencing coverage is required to apply this strategy; an average of 36M reads per sample was obtained; from those, around 55% were mapped to the host genome, and 42% was suitable for microbiome characterization. When there is no interest in host gene expression, strategies that reduce the host sequences can be applied to obtain a reliable microbiome, reducing the need for higher sequencing coverage and the implied costs.

In this work, *A. destruens* and *Phaeoacremonium* spp. were the most abundant GTD pathogens identified both through cultivation and metatranscriptomic approaches. Only in the case of KrakenUniq output, *N. parvum*, *D. corticola*, and *E. lata* were identified, although in all the samples in very low abundance (< 0.001 in relative abundance, TableS3.xlsx). This result requires further meticulous analysis, mainly because *E. lata* has never been isolated in the region. The only pathogen that was highly abundant in HDM symptomatic plants was *A. destruens*. Similar results were obtained for other GTD, indicating that it is impossible to differentiate SYM from ASYM plants based only on the presence of pathogens and the differencesdepends on their quantitative levels [11, 21–23]. Interestingly, *Phaeoacremonium* spp. and *P. chlamydospora*, regularly isolated from HDM plants [2, 6], were not identified in differential abundance, even by high sensitive molecular methods. Despite not differential, *Phaeoacremonium minimum* (formerly *P. aleophilum*) was present at low but detectable levels (> 0.0001 relative abundance) in all the samples,. This result, is in agreement with a previous report of *P. minimum* as a common isolate from SYM HDM plants [2]. *P. chlamydospora* was not detected by cultural isolation nor by molecular methods. *P. chlamydospora* has been mainly associated with young plants less than eight years old [30]. Since the plants sampled were around 23 years old, this could explain why *P. chlamydospora* was not detected at all. In any case, more work needs to be done to understand the role of *P. chlamydospora* in HDM disease.

For the prediction of antagonistic microorganisms to HDM pathogens, first, we suggested those with a negative correlation based on fungal presence/absence (Fig. 3). From this analysis, four fungi that belong to Pleosporales, *A. alternata*, *A. solani*, *P. nodorum*, and *D. pinodes* were identified. None of these four species have reported biological control ability; instead, they are pathogens of different hosts; therefore, it is risky to consider them for further BCA ability evaluation. A second strategy was to focus on those microorganisms showing a decrease in the microbiome in SYM plants, which could indicate that only in their absence or at low levels, the pathogen *A. destruens* can thrive and become the majority in the microbiome. Based on a bibliographic analysis, we discuss those microorganisms previously reported as BCAs or plant growth promoters (PGP). Three members of Archaea, *Halococcus* sp., *Halalkalicoccus* sp., and *Haloquadratum* sp. are proposed as candidates. Recently, it was determined that haloarchaea mediate phosphorous mobilizations, therefore, it could have a role as PGP [31–32]. Several Ascomycetes overrepresented in ASYM plants and underrepresented in SYM plants could have a role as BCAs. For instance, *Kretzchmaria deusta*,, is an endophyte of a variety of ash resistant to dieback caused by *Hymenoscyphu fraxineus* that can inhibit spore germination of the pathogen [33]; therefore further research on the interaction of *K. deusta* with *A. destruens* should be done. *Thichoderma* spp. are well recognized BCA and PGP in grapevine [34]. Our data showed several *Trichoderma* species but in low proportions. *Thrichoderma reesei* was more represented in ASYM plants c23 (> 0,001), suggesting it could be a good candidate for further biological control ability evaluation. Another Ascomycota previously found as BCA candidate for the GTD pathogen *Diplodia seriata* is *Aureobasidium pullulans* [35]. In the present work, *A. pullulans* was less represented (< 0.001), but *A. namibiae* and *A. subglaciale* were found in levels above 0.001, therefore could be further evaluated for the capacity to control GTD.

On the other hand, the prokaryotic microbiome indicates that Actinobacterias were differentially represented in symptomatic vines. Bruez et al. [22] and Elena et al. [36] explored the bacterial microbiome in Esca, but did not identify any BCA candidates. A role of Actinobacterias as BCA has been reported [37], but contrasting to our results, *Streptomyces* spp. (actinobacterias) were found antagonist to GTD pathogens, while our data showed they were mainly represented in SYM plants; therefore, a promoting disease role was assumed. Recently, it was proposed that the Actinobacteria/Bacteroidetes ratio in rhizosphere increases in domesticated plants with low tolerance to biotic and abiotic stress [38], suggesting that this ratio can help for monitoring the sanitary status of grapevine. *Flavobacterium commune* was the only bacteria identified with a significantly higher abundance in ASYM plants (Fig. 4). *Flavobacterium* sp. was reported to inhibit the germination of the GTD pathogen *Lasiodiplodia theobromae* [39]; therefore, a role as a BCA is hypothesized.

Grapevine gene expression and functional enrichment indicate that processes related to stress, as responses to unfolded protein, heat, drought, and nutrient deficiencies, are induced in symptomatic grapevines. This global response indicates that SYM plants are under stress, but it is not possible to determine if such stress is the result of the management of the vineyard or is due to a change in a microbiome that favors the colonization of *A. destruens*. Despite the triggering cause, it is clear that stress has a significant role in the appearance of symptoms. This was previously addressed [40], however to the best of our knowledge, it was never found using an integrative “in field” approach. Previous works evaluated the effect of stress on GTDs pathosystem using only one or two GTDs pathogens [41–43]; thus, this is the first time that all the complexity of agents involved in HDM disease in *Vitis vinifera* cv. Malbec is addressed in Argentinean field conditions. Results highlight the importance of avoiding stress on plants of local vineyards.

In Botryosphaeriaceae, abiotic stresses such as drought and heat were suggested as triggering factors for the endophyte-pathogen transition [44–45]. A recent review illustrates the hypothesis for GTD occurrence [40] based on those with direct effect (abiotic stress on the plant, pathogen, or both) and those with indirect effect (abiotic stress perturbing microbiome interactions). In this study we explored the microbiome and grapevine gene expression simultaneously. Polyamines are required for plants to deal with abiotic and biotic stress; therefore, it is difficult to understand why grapevine is repressing such functions in symptomatic plants. Also, microorganismscould synthesize polyamines. Therefore a pathogen hijacking strategy must not be discarded [46]. Probably in ASYM plants, polyamine synthesis is the main defense that restricts pathogen colonization.

From the microorganism's functional side, the TCA and TCA-glyoxylate bypass cycles are the main pathways activated on the microbial population hosted in SYM plants. The glyoxylate bypass allows the cell to synthesize glucose uniquely from acetate or dicarboxylic acid derived from fatty acid degradation [47]. This strategy could be fundamental to grow in a tissue with a considerable limitation of carbohydrates, such as grapevine vascular tissue, especially under stressful conditions because the plant redirects sugars toward the defense metabolic pathway. On the other side, a recent study indicates that microbes involved in hydrocarbon degradation are under oxidative stress, because of the sub-production of hydrogen peroxide during the oxidation of such compounds. In response to that environment, microbes upregulate glyoxylate shunt pathways to keep gluconeogenesis and growth working under such stressful conditions [47]. The degradation of aromatic compounds is required to deal with several components of grapevine woods such as pectin and lignin; therefore, it is quite probable that microorganisms are obligated to activate that pathway for survival.

Besides studying the host gene expression, we aimed to identify markers for the early detection of HDM disease. Due to the association of the disease with stress, it is essential to simultaneously quantify general stress marker expression and specific microorganism abundance, as a strategy to prevent HDM disease. Such markers will be beneficial, since periodic monitoring of vineyards along with preventative managing practices, would extend the production time of grapevines. We believe that one of the main findings of this study is the increased ratio of Basidiomycota/Ascomycota in SYM plants and the significantly increased polyamine biosynthesis in ASYM plants. Therefore specific quantification of such molecular markers must be developed and validated to be used as an indicator of early HDM stages or to detect levels of susceptibility to develop this disease.

Since only two plants were used for comparison of host gene expression and microbiome, conclusions must be taken with caution. Of course, more plants need to be analyzed to have higher confidence. However, the originality of this work has sustenance in the determination of microbiome from RNA derived reads allowing a higher resolution in terms of taxonomical "deepness" of classification than classical metabarcoding analyses.

We hope the approach here presented serves as a road-map to develop a more specific evaluation of the microbiome-pathogens-grapevine interactions in GTD.

Conclusions

The integral analysis of the multi-kingdommicrobiome with grapevine gene expression indicates that stress-responsive genes (through polyamine and trehalose synthesis) are the main factor explaining differences between symptomatic and asymptomatic plants. These findings support the previous suggestions to manage GTD using preventive practices that guaranteed the minimization of stress in the vines.

Methods

Sample collection

Plants of *Vitis vinifera* cv. Malbec of around 23 years-old on vertical trellis training system were collected at the end of winter from an experimental vineyard at Estación Experimental Agropecuaria INTA Mendoza in Luján de Cuyo, Mendoza, Argentina. The selection of plants for sampling was made based on the genotype (using the information of previous characterized cloning material) and the presence or absence of HDM symptoms. Five plants for each condition, symptomatic (SYM) and asymptomatic (ASYM), were collected and taken immediately to the laboratory. After surface cleaning of the cortex with 70% ethanol, several slices were obtained at three different positions in the trunk and both arms. While cutting the plant, the resulting woodchips were collected into a clean, sterile plastic bag and immediately stored at -80 °C until RNA extraction. After each cut, the saw was carefully cleaned with 70% ethanol and 3% hydrogen peroxide.

Microbial Culture Isolation

Thin slides obtained from the base and close to the head of the trunk and the arms were sawed. For each sample, five pieces of wood were placed onto malt extract agar (MEA) medium in Petri dishes. Plates were incubated at 24 °C, monitored daily, and after one week, evaluated for morphological characterization. Observed bacterial or fungal growth was replicated onto fresh MEA medium and incubated at 24 °C again. Cultures grown in MEA were initially classified based on the macroscopic mycelium characteristics, including colony shape, texture, color, and microscopic features, including shape and color of mycelia, and shape of the conidia. The identified microorganisms were counted per sample and per isolates, considering the pure cultures to estimate the abundance.

Rna Extraction And Sequencing

Three SYM and three ASYM plants were selected for RNAsEq. A pool of grapevine woodchip was obtained and ground with a mortar and liquid nitrogen. Around 400 mg of the resulting powder was used for RNA extraction, adapted from Chang et al., [48] in 15 mL centrifuge tubes. Briefly, the grapevine powder was incubated with cetyl trimethyl ammonium bromide (CTAB) extraction buffer after incubation at 65 °C for 10 min, a Chloroform:Isopropyl alcohol mixture (24:1) was added and after centrifugation, the aqueous phase was recovered. Then a precipitation step using 3M pH 8 sodium acetate was done, and the RNA was precipitated with 10M lithium chloride. Finally, two washing steps with 75% ethanol were included. Total RNA obtained was treated with RQ1 Promega DNAse to eliminate contaminant DNA, and RNA cleaning was done with R1015 Zymo Clean and Concentration kit following the manufacturer's recommendations.

Total RNA was quantified in a Nanodrop2000, and its integrity was determined in 1.5% agarose gel. Library preparation was done through TruSeq® Stranded Total RNA Library Preparation Kit with Ribo-Zero™ and sequencing in Illumina HiSeq4000 2 × 100 bp in Macrogen, Inc. (South Korea).

Bioinformatics Analyses

The analyses were done in the computational HPC at CICESE (Ensenada, Baja California, Mexico). The pipeline schema is described in FigureS7.pdf and a guide with details is provided in [49].

Trimming, Grapevine Gene Expression, And Functional Enrichment Analysis

Fastqc v0.11.7 [50] was used for general quality analysis. Trimmomatic v0.38 [51] was used for clipping out TruSeq3-PE-2 adapters through the next parameters: 'TruSeq3-PE-2.fa:2:30:10 SLIDINGWINDOW:4:15 LEADING:5 TRAILING:5 MINLEN:25'. STAR v2.6.1 [52] was used for mapping the trimmed reads on *Vitis vinifera* cv. Pinot Noir genome (12X, ENSEMBL release-41). The mapped reads were counted for each gene using the STAR parameter '–quantMode GeneCounts', and a matrix of counts for all the samples was constructed through build_count_matrix.R script (described in [49]).

The mapped read counts matrix was used for edgeR v3.20.9 analysis. Based on the similarity of microbial composition samples c23 and c25 were used as “controls” while samples m11 and m26 were used as “symptomatic”. When only those samples were used, several differentially expressed genes (degs) were found. GO terms enrichment was evaluated for degs list through Goseq v1.32.0 [53]; the output of enrichment was used to make plots through Goplot v1.0.2 [54].

Plant Rrna And Organelle Reads Remotion

Although the libraries were constructed using Plant Ribo-Zero, remaining plant rRNA reads in the SortMeRNA v2.0 [55] output file were identified. To remove plant rRNA reads, the most abundant rRNA from *Arabidopsis thaliana* was used as a query in NCBI blast. The complete sequences of the best 100 hits were downloaded and, after manual editing, used as a reference in bowtie2 v2.3.4.3 [56] mapping. Similarly, to remove all reads that map on the plastid and mitochondrial genome, the organelle sequences of all the organisms available at Refseq [57], together with DNA and RNA DB from plastids [58] and mitochondrion [59] were downloaded and used as a reference in bowtie2 v2.3.4.3 [56] mapping. The remaining filtered reads were used for microbial composition analysis.

Microbiome Analysis

Because of the recent development of bioinformatics tools to process metatranscriptomic data, there are no clear delineations or consensus regarding what is the best tool for characterization of the microbiome composition from metatranscriptomic derived data. In this work, three alternatives were carried out. The first was using MATAM v1.5.3 [60] to identify all the rRNA derived reads (except those from plants that were previously removed) and reconstruct the phylogenetic marker gene through a reference-guided assembly strategy. The second was through the use of KrakenUniq v0.5.7 [61] that takes all the trimmed and filtered reads for k-mer indexing as input and then map the k-mer in nucleotide microbial DB and use the unique k-mer counts for relative abundance estimations. The last was through the use of Humann2 v0.11.2 [62] that use marker DB as a reference, and later construct pangenomes reference only with the microorganisms previously identified for a more in-depth taxonomic characterization in a more manageable microbial part of ‘nt’ NCBI DB.

Matam Assembly With Prokaryotic-16s-silva And Fungal Its-rdp Model

The unmapped reads on *Vitis vinifera* cv. Pinot Noir genome filtered to remove remaining plant rRNA and organelle derived reads, as explained before, were used for mapping and reconstruction of ribosomal regions and comparison on SILVA-SSU-DB [63] for prokaryotic, SILVA-LSU-DB [63] for eukaryotic, and ITS-RDP [29] for fungal classification, through MATAM v1.5.3 [60]. In the case of the Warcup_RDP_ITS DB [28], the threshold for clustering reference sequences was set to 200 bp when running matam_db_preprocessing.py script, and when running the assembly, the minimal scaffold length was set to 200 bp.The training model for the assembly was specified as “fungalits_warcup”.

Unique k-mers used for the whole classification and relative abundance quantification

KrakenUniq v0.5.7 [60] was used for splitting the grapevine genome unmapped reads in kmers of 31 bp length and directly mapping on the microbial part of NCBI ‘nt’ DB [29]. It contains 14,772,991 sequences that correspond mainly to the Bacteria superkingdom (6,549,136 sequences), Fungi Kingdom (3,836,040 sequences), Virus superkingdom (2,050,013 sequences) and Archaea superkingdom (326,186 sequences). All taxa in the DB contain 1,355,495 species [64]. The principle to estimate relative abundance derives from counting the number of unique identified k-mers in each taxon through the use of cardinality estimation algorithm HyperLogLog. In this manner, it is possible to count how many genome-unique k-mers are covered by reads, allowing the discernment of true from false positives.

Microbial gene expression and differential (SYM vs ASYM) metabolic pathways identification

The unmapped and filtered reads of *V. vinifera* genome were used for processing through Humann2 v0.11.2 [62]. This pipeline was developed in the framework of the Human Microbiome Project (HMP) [65] to extract functional information from the metagenome or metatranscriptome data collected from the microbiome in human tissues, and here it was adapted for grapevine. First taxonomic identification was done through mapping on a cluster of marker genes for several microorganisms using MetaPhlan DB [66]. MetaPhlan DB is constituted by unique clade-specific marker genes identified from 17,000 reference genomes (13,500 bacterial and archaeal; 3,500 viral, and 110 eukaryotic) [65]. The organisms identified were used as a list for selecting the pangenome in Chocophlan DB [62] and then used as a reference for mapping in the second step, while the unmapped reads in the first step were processed through diamond against UniRef90 DB [67]. At the end, the counts of reads were grouped by gene families (GF) or metabolic pathways (through the relationship GF-MetaCyc DB [68]). Statistical comparison between treatments was done using Kruskal-Wallis on the raw counts of pathways for each sample to construct a joined table (humann2_join_table function) and testing for differential expression based on edgeR statistics.

Nucleotide Sequence Accession Number

The data was deposited on ENA-EMBL under the project registered as PRJEB31098.

List Of Abbreviations

CTAB: Cetyl Trimethyl Ammonium Bromide

GTD: Grapevine Trunk Diseases

HDM: ‘Hoja de malvón’

ASYM: asymptomatic

SYM: Symptomatic

HTS: High Throughput Sequencing

SSCP: Single Strand Conformational Polymorphism

ITS: Internal Transcribed Sequence

SSU: Small Ribosomal Subunit

LSU: Large Ribosomal Subunit

RDP: Ribosomal Database Project

BCA: Biological Control Agent

PGP: Plant Growth Promotion

MEA: Malt Extract Agar

HPC: High Performance Computing

NCBI: National Center for Biotechnological Information

GF: Gene families

DB: Database

EBI-EMBL: European Bioinformatics Institute-European Molecular Biology Laboratory

Declarations

Ethics approval and consent to participate

Not applicable

Consent for publication

Not applicable.

Availability of data and materials

The dataset supporting the conclusions of this article is available in the ENA-EMBL repository, [PRJEB31098 https://www.ebi.ac.uk/ena/data/view/PRJEB31098]

Competing interest

The authors declare that they have no competing interests

Funding

This research was supported by Instituto Nacional de Tecnología Agropecuaria through the 'Proyecto Regional con Enfoque Territorial-Desarrollo territorial del Oasis Norte de Mendoza-PRET-1251101 (2013 – 2019)'. MP acknowledges the support by the Argentine National Council of Scientific and Technical Research (CONICET) postdoctoral fellowship.

Author's contribution

MCC, MGE, and MP designed the experiment and performed the collection of samples. MCC made the isolation of fungus through classical methods. MP made RNA extraction, managed the experimental design for NGS, performed bioinformatics analyses, and wrote the manuscript. MCC, MGE, SGL, RHM contribute to manuscript revision. All authors read and approved the final manuscript

Acknowledgments

We acknowledge to Clara Elizabeth Galindo-Sanchez for kindly sharing the CICESE HPC resources and to Sylvia Camacho Lara for all the informatics administration support required for this work. Thanks to Luciana Garcia from Instituto Nacional de Vitivinicultura (INV) for sharing the Nanodrop2000 required for RNA quantification.

References

1. Gramaje D, Úrbez-Torres JR, Sosnowski MR. Managing Grapevine Trunk Diseases With Respect to Etiology and Epidemiology: Current Strategies and Future Prospects. Plant Dis. 2018; https://doi.org/10.1094/PDIS-04-17-0512-FE

2. Gatica M, Dubos B, Larignon P. The “hoja de malvón” grape disease in Argentina. Phytopathol Mediterr. 2000; 39:41–45.

3. Gatica M, Césari C, Escoriaza G. Phellinus species inducing hoja de malvón symptoms on leaves and wood decay in mature field-grown grapevines. Phytopathol Mediterr. 2004; 43:59-65.

4. Aguilera-Vega NA. Identificación de la especie Hymenomycete (Basidiomycota) asociada a síntomas de enrollamiento clorótico de la vid (Vitis vinifera L) en Chile. Tesis de Maestría. Universidad de Chile; 2004.

5. Fischer M, Gonzalez-Garcia V. An annotated checklist of European basidiomycetes related to white rot of grapevine (Vitis vinifera). Phytopathol Mediterr. 2015;54: 241-52. https://doi.org/10.14601/Phytopathol

6. Lupo S, Bettucci L, Pérez A, Martínez S, Césari C, Escoriaza G, et al. Characterization and identification of the basidiomycetous fungus associated with “hoja de malvón” grapevine disease in Argentina. Phytopathol Mediterr. 2006;45:110-16.

7. Pildain MB, Pérez GA, Robledo G, Pappano DB, Rajchenberg M. Arambarria the pathogen involved in canker rot of Eucalyptus, native trees wood rots and grapevine diseases in the Southern Hemisphere. For Pathol. 2017;47: 1–12. https://doi.org/10.1111/efp.12397

8. Informes Anuales. Instituto Nacional de Vitivinicultura. 2019 https://www.argentina.gob.ar/inv/vinos/estadisticas/superficie/anuarios

9. Úrbez-Torres JR, Haag P, Bowen P, Lowery T, O’Gorman DT. Development of a DNA macroarray for the detection and identification of fungal pathogens causing decline of young grapevines. Phytopathology. 2015; 105:1373–88. https://doi.org/10.1094/PHYTO-03-15-0069-R

10. Pouzoulet J, Rolshausen PE, Schiavon M, Bol S, Travadon R, Lawrence DP, et al. A method to detect and quantify Eutypa lata and Diplodia seriata-Complex DNA in Grapevine Pruning Wounds. Plant Dis. 2017; https://doi.org/10.1094/PDIS-03-17-0362-RE

11. Morales-Cruz A, Allenbeck G, Figueroa-Balderas R, Ashworth VE, Lawrence DP, Travadon R, et al. Closed-reference metatranscriptomics enables in planta profiling of putative virulence activities in the grapevine trunk disease complex. Mol Plant Pathol. 2018;19:490-503. https://doi.org/10.1111/mpp.12544

12. Casieri L, Hofstetter V, Viret O, Gindro K. Fungal communities living in the wood of different cultivars of young Vitis vinifera plants. Phytopathol Mediterr. 2009;48: 73–83.

13. González V, Tello, ML. The endophytic mycota associated with Vitis vinifera in central Spain. Fungal Divers. 2011; 47:29–42. https://doi.org/10.1007/s13225-010-0073-x

14. Pacifico D, Squartini A, Crucitti D, Barizza E, Lo Schiavo F, Muresu R, et al. The role of the endophytic microbiome in the grapevine response to environmental triggers. Front Plant Sci. 2019;https://doi.org/10.3389/fpls.2019.01256

15. Pinto C, Pinho D, SousaS, Pinheiro M, Egas C, Gomes AC. Unravelling the diversity of grapevine microbiome. PLoS One. 2014; :e85622.https://doi.org/10.1371/journal.pone.0085622

16. Salvetti E, Campanaro S, Campedelli I, Fracchetti F, Gobbi A, Tornielli GB, et al. Whole-metagenome-sequencing-based community profiles of Vitis vinifera L. cv. Corvina berries withered in two post-harvest conditions. Front Microbiol. 2016; 7:937. https://doi.org/10.3389/fmicb.2016.00937

17. Mezzasalma V, Sandionigi A, Guzzetti L, Galimberti A, Grando MS, Tardaguila J,et al. Geographical and cultivar features differentiate grape microbiota in Northern Italy and Spain vineyards. Front Microbiol. 2018;9:1–13. https://doi.org/10.3389/fmicb.2018.00946

18. Dissanayake AJ, Purahong W, Wubet T, Hyde KD, Zhang W, Xu H, et al. Direct comparison of culture-dependent and culture-independent molecular approaches reveal the diversity of fungal endophytic communities in stems of grapevine (Vitis vinifera). Fungal Divers. 2018; 90: 85-107. https://doi.org/10.1007/s13225-018-0399-3

19. Marasco R, Rolli E, Fusi M, Michoud G, Daffonchio D. Grapevine rootstocks shape underground bacterial microbiome and networking but not potential functionality. Microbiome. 2018;6:3. https://doi.org/10.1186/s40168-017-0391-2

20. Vitulo N, Lemos WJF, Calgaro M, Confalone M, Felis GE, Zapparoli G, et al. . Bark and grape microbiome of Vitis vinifera: influence of geographic patterns and agronomic management on bacterial diversity. FrontMicrobiol. 2018;9: 3203. https://doi.org/10.3389/fmicb.2018.03203

21. Hofstetter V, Buyck B, Croll D, Viret O, Couloux A, Gindro K. What if esca disease of grapevine were not a fungal disease? Fungal Divers. 2012; 54: 51–67.https://doi.org/10.1007/s13225-012-0171-z

22. Bruez E., Haidar R, Alou MT, Vallance J, Bertsch C, Mazet F, Bacteria in a wood fungal disease: characterization of bacterial communities in wood tissues of esca-foliar symptomatic and asymptomatic grapevines. Front Microbiol. 2015; 6: 1137. https://doi.org/10.3389/fmicb.2015.01137.

23. Bruez E, Baumgartner K, Bastien S, Travadon R, Guérin-Dubrana L, Rey P, et al. Various fungal communities colonise the functional wood tissues of old grapevines externally free from grapevine trunk disease symptoms. Aust J Grape Wine R.2016; https://doi.org/10.1111/ajgw.12209

24. Travadon R, Lecomte P, Diarra B, Lawrence DP, Renault D, Ojeda H, et al. Grapevine pruning systems and cultivars influence the diversity of wood-colonizing fungi. Fungal Ecol. 2016; 24:82–93. https://doi.org/10.1016/j.funeco.2016.09.003

25. Pinto C, Gomes AC. Vitis vinifera microbiome: from basic research to technological development. BioControl. 2016; https://doi.org/10.1007/s10526-016-9725-4

26. Kraus C, Voegele RT, Fischer M. Temporal development of the culturable, endophytic fungal community in healthy grapevine branches and occurrence of GTD-associated fungi. Microb Ecol. 2018; 1–11. https://doi.org/10.1007/s00248-018-1280-3

27. Nerva L, Zanzotto A, Gardiman M, Gaiotti F, Chitarra W. Soil microbiome analysis in an ESCA diseased vineyard. Soil Biol Biochem. 2019; 135, 60–70. https://doi.org/10.1016/j.soilbio.2019.04.014

28. Deshpande V, Wang Q, Greenfield P, Charleston M, Porras-Alfaro A, Kuske CR, et al. Fungal identification using a Bayesian classifier and the Warcup training set of internal transcribed spacer sequences. Mycologia. 2016; 108:1–5. https://doi.org/10.3852/14-293

29. NT DB ftp://ftp.ccb.jhu.edu/pub/software/krakenuniq/Databases/nt/ (downloaded 3/28/2018)

30. Sidoti A, Buonocore E, Serges T, Mugnai L. Decline of young grapevines associated with Phaeoacremonium chlamydosporum in Sicily (Italy). Phytopathol Mediterr. 2000; 39:87–91. https://doi.org/10.14601/Phytopathol_Mediterr-1533

31. Yadav AN, Verma P, Kaushik R, Dhaliwal HS, Saxena AK. Archaea endowed with plant growth promoting attributes. EC Microbiol. 2017; 6:294–298.

32. Etesami H, Beattie GA. Mining halophytes for plant growth-promoting halotolerant bacteria to enhance the salinity tolerance of non-halophytic crops. Front Microbiol. 2018; https://doi.org/10.3389/fmicb.2018.00148

33. Schlegel M, Dubach V, von Buol L, Sieber TN. Effects of endophytic fungi on the ash dieback pathogen. FEMS Microbiol Ecol. 2016; 92. https://doi.org/10.1093/femsec/fiw142

34. Mondello V, Songy A, Battiston E, Pinto C, Coppin C, Trotel-Aziz P, et al. Grapevine trunk diseases: a review of fifteen years of trials for their control with chemicals and biocontrol agents. Plant Dis. 2017; https://doi.org/10.1094/PDIS-08-17-1181-FE

35. Pinto C, Custódio V, Nunes M, Songy A, Rabenoelina F, Courteaux B, et al. Understand the potential role of Aureobasidium pullulans, a resident microorganism from grapevine, to prevent the infection caused by Diplodia seriata. Front Microbiol. 2018; 9:1-15. https://doi.org/10.3389/fmicb.2018.03047

36. Elena G, Bruez E, Rey P, Luque J. Microbiota of grapevine woody tissues with or without esca-foliar symptoms in northeast Spain. Phytopathol Mediterr. 2018; 57:425-438. https://doi.org/10.14601/Phytopathol

37. Álvarez-Pérez JM, González-García S, Cobos R, Olego MÁ, Ibañez A, Díez-Galán A, et al. Use of endophytic and rhizosphere actinobacteria from grapevine plants to reduce nursery fungal graft infections that lead to young grapevine decline. Appl Environ Microbiol. 2017; 83. https://doi.org/10.1128/AEM.01564-17

38. Pérez-Jaramillo JE, Carrión VJ, de Hollander M, Raaijmakers JM. The wild side of plant microbiomes. Microbiome. 2018; 6:143. https://doi.org/10.1186/s40168-018-0519-z

39. Gunasinghe WK, Karunaratne AM. Interactions of Colletotrichum musae and Lasiodiplodia theobromae and their biocontrol by Pantoea agglomerans and Flavobacterium sp. in expression of crown rot of “Embul” banana. BioControl. 2009; 54:587-596. https://doi.org/10.1007/s10526-009-9210-4

40. Songy A, Fernandez O, Clément C, Larignon P, Fontaine F. Grapevine trunk diseases under thermal and water stresses. Planta. 2019; https://doi.org/10.1007/s00425-019-03111-8

41. Sosnowski M, Luque J, Loschiavo AP, Martos S, Garcia-Figueres F, Wicks TJ, et al. Studies on the effect of water and temperature stress on grapevines inoculated with Eutypa lata. Phytopathol Mediterr. 2011;50:127-38.

42. van Niekerk JM, Strever E, Toit PG, Halleen F. Influence of water stress on Botryosphaeriaceae disease expression in grapevines. Phytopathol Mediterr; 50: 151-65.

43. Paolinelli-Alfonso M, Villalobos-Escobedo JM, Rolshausen P, Herrera-Estrella A, Galindo-Sánchez C, López-Hernández JF, et al. Global transcriptional analysis suggests Lasiodiplodia theobromae pathogenicity factors involved in modulation of grapevine defensive response. BMC Genomics. 2016; 17:615. https://doi.org/10.1186/s12864-016-2952-3

44. Félix C, Duarte AS, Vitorino R, Guerreiro ACL, Domingues P, Correia ACM, et al. Temperature modulates the secretome of the phytopathogenic fungus Lasiodiplodia theobromae. Front Plant Sci. 2016; 7:1096. https://doi.org/10.3389/fpls.2016.01096

45. Qiu Y, Steel CC, Ash GJ, Savocchia S. Effects of temperature and water stress on the virulence of Botryosphaeriaceae spp. causing dieback of grapevines and their predicted distribution using CLIMEX in Australia. Acta Hortic. 2016; 1115:171-81. https://doi.org/10.17660/ActaHortic.2016.1115.26

46. Jiménez-Bremont JF, Marina M, Guerrero-González ML, Rossi FR, Sánchez-Rangel D, Rodríguez-Kessler M, et al. Physiological and molecular implications of plant polyamine metabolism during biotic interactions. Front Plant Sci. 2014; 5: 95. https://doi.org/10.3389/fpls.2014.00095

47. Ahn S, Jung J, Jang IA, Madsen EL, Park W. Role of glyoxylate shunt in oxidative stress response. J Biol Chem. 2016; 291:11928–11938. tps://doi.org/10.1074/jbc.M115.708149

48. Chang S, Puryear J, Cairney J. A simple and efficient method for isolating RNA from pine trees. Plant Mol Biol Rep. 1993; 11:113–116. https://doi.org/10.1007/BF02670468

49. Guide for bioinformatic analysis in the current work https://bitbucket.org/quetjaune/rnaseq_malbec_082018/src/master/Malbec_metatranscriptomic_analysis.md

50. FastQC https://www.bioinformatics.babraham.ac.uk

51. Trimmomatic (http://www.usadellab.org/cms/?page=trimmomatic)

52. Dobin A, Gingeras TR. Mapping RNA-seq reads with STAR. Curr Protoc Bioinformatics. 2015; 51:1-19. https://doi.org/10.1002/0471250953.bi1114s51. https://github.com/alexdobin/STAR

53. Young MD, Wakefield MJ, Smyth GK, Oshlack A. Gene ontology analysis for RNA-seq: accounting for selection bias. Genome Biol. 2010; 11:R14. https://doi.org/10.1186/gb-2010-11-2-r14

54. Walter W, Sanchez-Cabo F, Ricote M. GOplot: an R package for visually combining expression data with functional analysis. Bioinformatics. 2015; 2912-14. https://doi.org/10.1093/bioinformatics/btv300

55. Kopylova E, Noé L, Touzet H. SortMeRNA: Fast and accurate filtering of ribosomal RNAs in metatranscriptomic data. Bioinformatics. 2012; 28:3211–3217. https://doi.org/10.1093/bioinformatics/bts611

56. Langmead B, Salzberg SL. Fast gapped-read alignment with Bowtie 2. Nature Methods. 2012; 9:357–359. https://doi.org/10.1038/nmeth.1923

57. RefSeq organelle (https://www.ncbi.nlm.nih.gov/genome/organelle/)

58. RefSeq plastid (ftp://ftp.ncbi.nlm.nih.gov/refseq/release/plastid/)

59. RefSeq mitochondrion (ftp://ftp.ncbi.nlm.nih.gov/refseq/release/mitochondrion/)

60. Pericard P., Dufresne Y, Couderc L, Blanquart S, Touzet H. MATAM: Reconstruction of phylogenetic marker genes from short sequencing reads in metagenomes. Bioinformatics. 2018; 34:585–591. https://doi.org/10.1093/bioinformatics/btx644

61. Breitwieser FP, Baker DN, Salzberg SL KrakenUniq: confident and fast metagenomics classification using unique k-mer counts. Genome Biol. 2018;19:198. https://doi.org/10.1186/s13059-018-1568-0

62. Franzosa EA, McIver L J, Rahnavard G, Thompson LR, Schirmer M, Weingart G, et al. Species-level functional profiling of metagenomes and metatranscriptomes. Nat Methods. 2018; 15:962-68. https://doi.org/10.1038/s41592-018-0176-y

63. Quast C, Pruesse E, Yilmaz P, Gerken J, Schweer T, YarzaP, et al. The SILVA ribosomal RNA gene database project: Improved data processing and web-based tools. Nucleic Acids Res. 2013; https://doi.org/10.1093/nar/gks1219

64. Breitwieser FP, Lu J, Salzberg SL. A review of methods and databases for metagenomic classification and assembly. Brief Bioinform. 2018; 20:1125-39. https://doi.org/10.1093/bib/bbx120

65. Human Microbiome Project https://portal.hmpdacc.org/

66. MetaPhlan Database http://huttenhower.sph.harvard.edu/metaphlan

67. Suzek BE, Wang Y, Huang H, McGarvey PB, Wu CH. UniRef clusters: a comprehensive and scalable alternative for improving sequence similarity searches. Bioinformatics. 2015; 31: 926-32. https://doi.org/10.1093/bioinformatics/btu739

68. Caspi R, Billington R, Fulcher CA, Keseler IM, Kothari A, Krummenacker M, et al. The MetaCyc database of metabolic pathways and enzymes. Nucleic Acids Res. 2018; 46:633–639. https://doi.org/10.1093/nar/gkx935

Additional Files

Additional file 1: TableS1.xlsx Isolated microorganisms characterized by morphological aspects. The relative abundance was calculated based on the numbers of isolates for each taxon and calculating the ratio to total numbers of all the isolates.

Additional file 2: TableS2.xlsx Main sequencing results and primary processing of RNAseq data

Additional file 3: FigureS1.html Microbiome prokaryotic composition determined through 16S marker reconstruction. The counts of reads in each reconstructed and classified through MATAM software were used for the construction of Krona plots for each sample. ASYM (c22, c23, c25) and SYM (m11, m16, m26).

Additional file 4: FigureS2.html Microbiome eukaryotic composition determined through LSU marker reconstruction. The counts of reads in each reconstructed marker and classified through MATAM software were used for the construction of Krona plots for each sample. ASYM (c22, c23, c25) and SYM (m11, m16, m26).

Additional file 5: FigureS3.html Microbiome fungal composition determined through ITS marker reconstruction. The counts of reads in each reconstructed marker and classified through MATAM software were used for the construction of Krona plots for each sample. ASYM (c22, c23, c25) and SYM (m11, m16, m26).

Additional file 6: FigureS4.html 'Whole' microbiome composition determined through unique kmer identification. The unique kmers were used for taxa identification and through KrakenUniq software, then the counts for each unique kmer were used for the construction of Krona plots for each sample. ASYM (c22, c23, c25) and SYM (m11, m16, m26).

Additional file 7: TableS3.xlsx 'Whole' microbiome composition determined through unique kmer identification. The raw unique kmer counts matrix obtained from KrakenUniq output.

Additional file 8: FigureS5.pdf Non-metric multidimensional scaling plot separated for Bacteria and Eukaryota obtained from KrakenUniq output data. The counts for each classified taxa on each sample were used to calculate Bray Curtis distances and then to graph a dimensionless plot. Bacteria data show no pattern of counts based on classification, but the Basidiomycota classification got a similar pattern of counts and contrasting to Ascomycota classified reads.

Additional file 9: FigureS6.pdf Non-metric multidimensional scaling plot obtained from KrakenUniq output data. The counts for each classified taxa on each sample were used to calculate Bray Curtis distances and then to graph the dimensionless plot. No clustering of 'replicates' was obtained. Based on this graph and the previous observation of *A. destruens* isolated in sample c22, this sample was removed for further statistic SYM vs. ASYM comparison. Sample m16, despite clearly HDM symptomatic, was discarded for statistic comparison because of the marked advance of the symptoms respect to m11 and m26.

Additional file 10: TableS4.xlsx edgeR statistical test result for SYM vs. ASYM microorganism abundance.

Additional file 11: TableS5.xlsx Relative abundance of expressed microbial pathways obtained from humann2 output.

Additional file 12: TableS6.xlsx edgeR statistical test result for SYM vs. ASYM *Vitis vinifera* cv. Malbec gene expression.

Additional file 13: FigureS7.pdf Bioinformatics analysis schema. The quality filtering was done through Trimmomatic v0.38, mapping of high quality reads on *Vitis vinifera* cv. Pinot Noir genome PN40024 was done with Star v2.6.1. Mapped and counted reads in Star were used to calculate grapevine gene expression and then comparing SYM vs. ASYM samples. The list of differential expressed genes was used to interrogate for functional enrichment through GOseq v1.32.0 based on Gene Ontology categories. In the case of unmapped reads in the grapevine genome, an extra filter step was included to remove all the reads having homology with *A. thaliana* rRNA and plant organelles. The remaining reads were used for microbiome characterization with alternative methods: one that based on phylogenetic marker reconstruction through MATAM v1.5.3, the other was using the unique kmer counts throughKrakenUniq v0.5.7 and finally for microbial functional analysis through the use of Humann2 v0.11.2. For details of scripts used check https://bitbucket.org/quetjaune/rnaseq_malbec_082018/src/4a26e618215c3729f81a3b935942066d5573d011/Malbec_metatranscriptomic_analysis.md

Figures

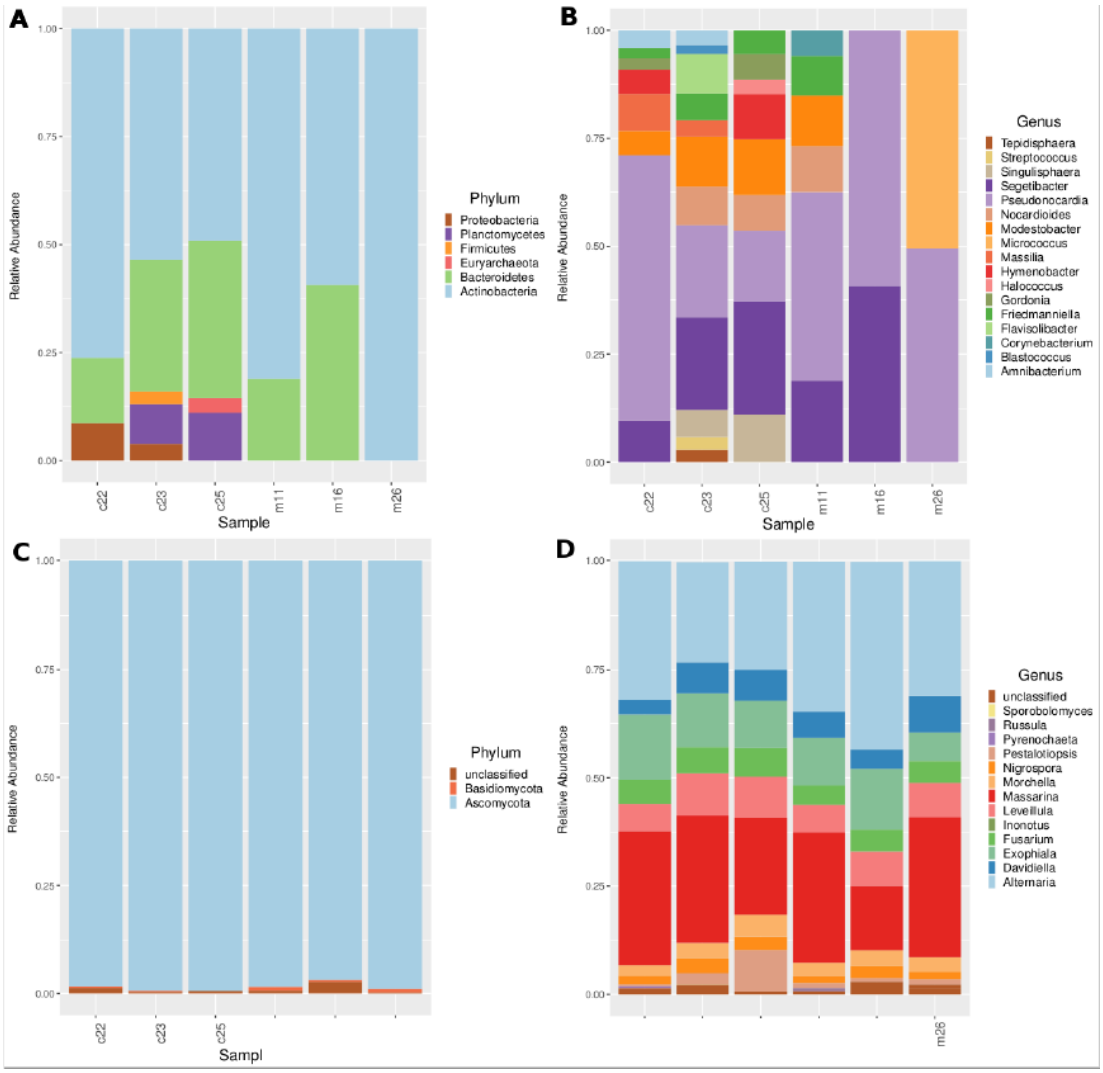

Figure 1

Prokaryotic and fungal microbiome Vitis vinifera cv. Malbec. The relative abundance of prokaryotic microorganisms identified through MATAM 16S rRNA reconstruction at Phylum (A) and Genus (B) taxonomic levels. The relative abundance of fungi identified through MATAM ITS rRNA reconstruction at Phylum (C) and Genus (D) taxonomic level.

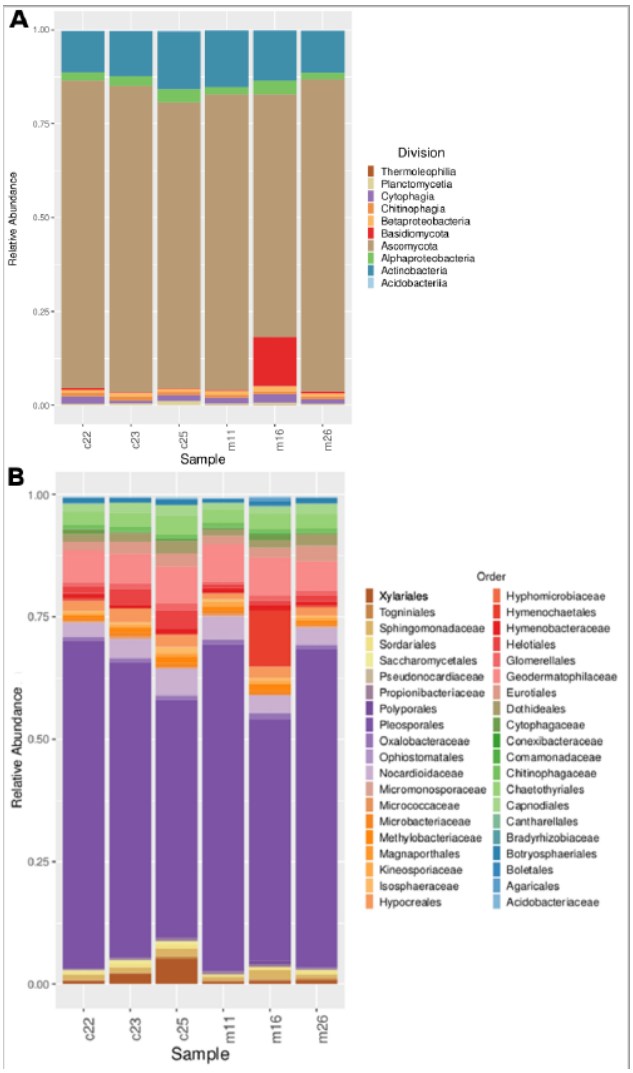

Figure 2

Multi-kingdom microbiome in Vitis vinifera cv. Malbec based on unique kmers counts. Relative abundance calculated by different taxonomic ranges: Division (A) and Order (B).

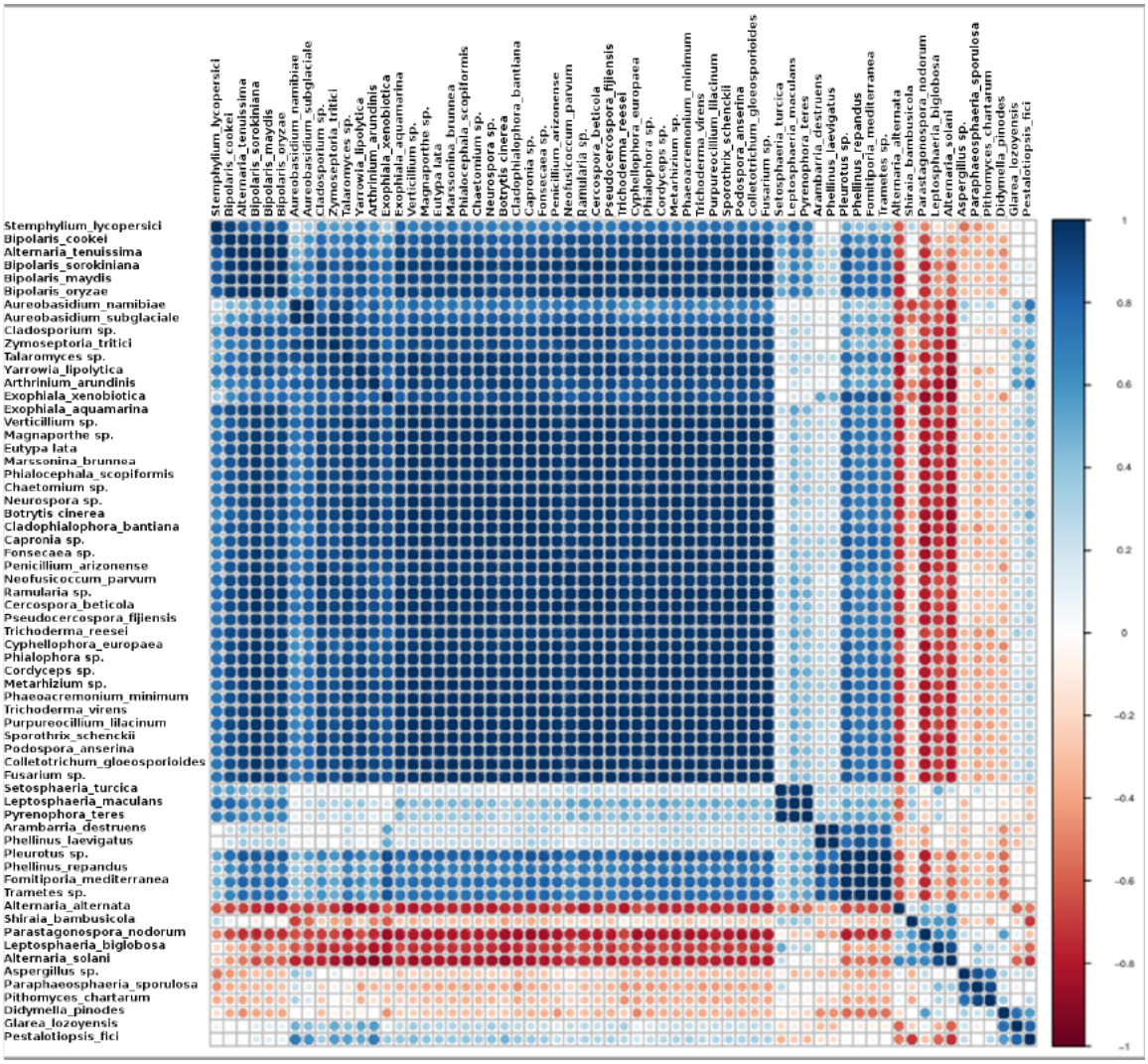

Figure 3

Interactions between members of the fungal community of the grapevine microbiome. Positive (trends to blue) and negative (trends to red) correlations among highly abundant fungi identified through unique kmers using KrakenUniq software. The "Hoja de malvón" pathogen Arambarria destruens have negative interactions with three members of Pleosporales order: Alternaria alternata, Parastagonospora nodorum, and Didymella pinodes. Another pathogen Phaeoacremonium minimum has negative interactions with the same fungal community as negatively interacts with Arambarria destruens, Leptosphaeria biglobosa, and Alternaria solani.

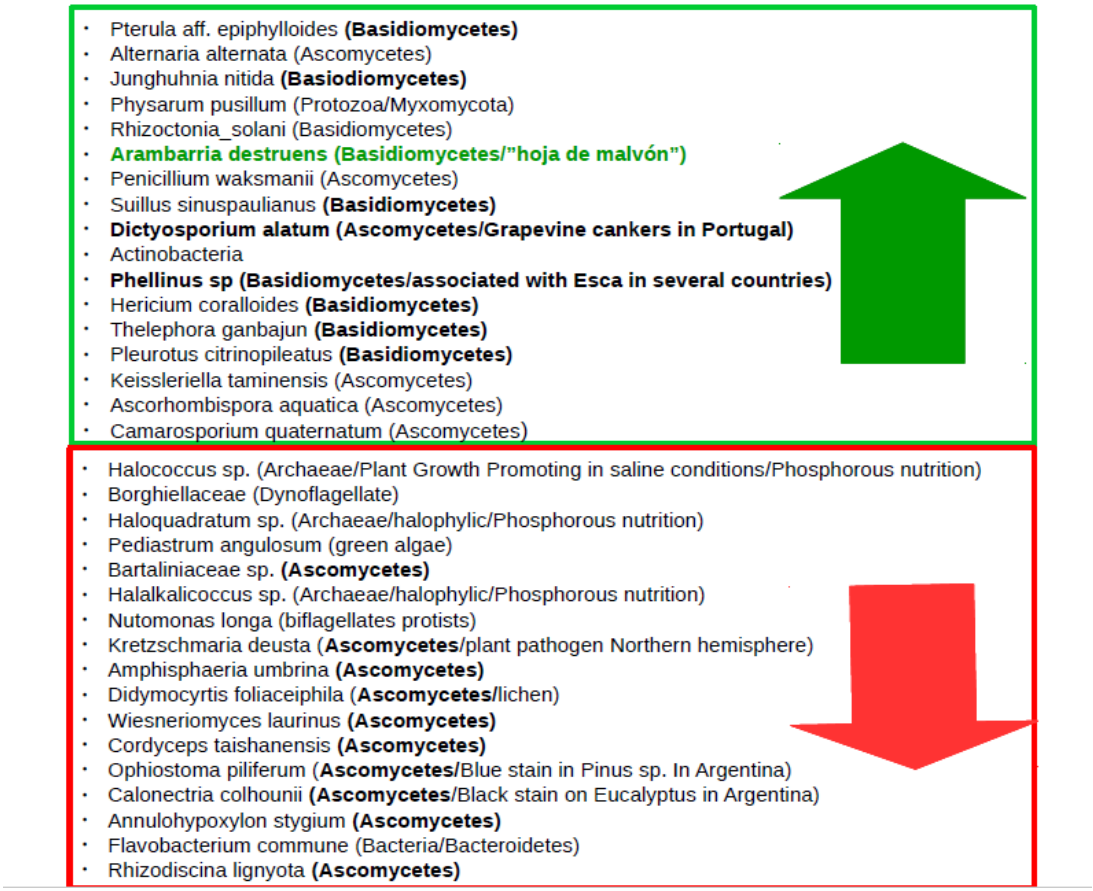

Figure 4

Differential microorganisms obtained in SYM vs. ASYM comparisons. Using the unique KrakenUniq output data, a table count was constructed, and differential microorganisms identified based on edgeR statistical method (FDR<0.15). Microorganisms with higher abundance in SYM/ASYM are shown in the green box, while those in lower abundance in SYM/ASYM are shown in the red box. The results from edgeR statistic test are in TableS4.xlsx

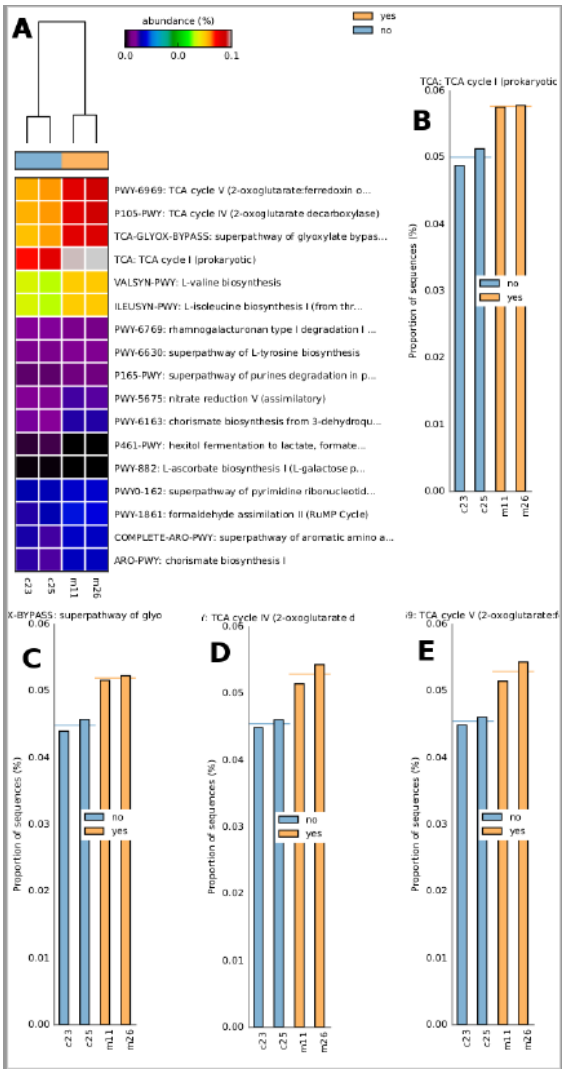

Figure 5

Microbial functional pathways in SYM vs. ASYM comparison. Using humann2 the main abundant microorganisms were identified through a multi-marker strategy, a pangenome (only having the identified microorganisms) was constructed to be used as a reference for mapping the raw reads of each sample. Counts of mapped reads on genes grouped through the MetaCyc pathways database were used to calculate significant differences through the ANOVA Tukey-Kramer test (p-value<0.05). A) Heatmap showing the main differential pathways. B), C), D), and E) corresponds to bar plots from TCA cycles-associated pathways. The bypass of the glyoxylate cycle might indicate that microorganisms with great functional activities activate a process of anabolism from lipids and/or amino acids that could be available because of host cell disruption.

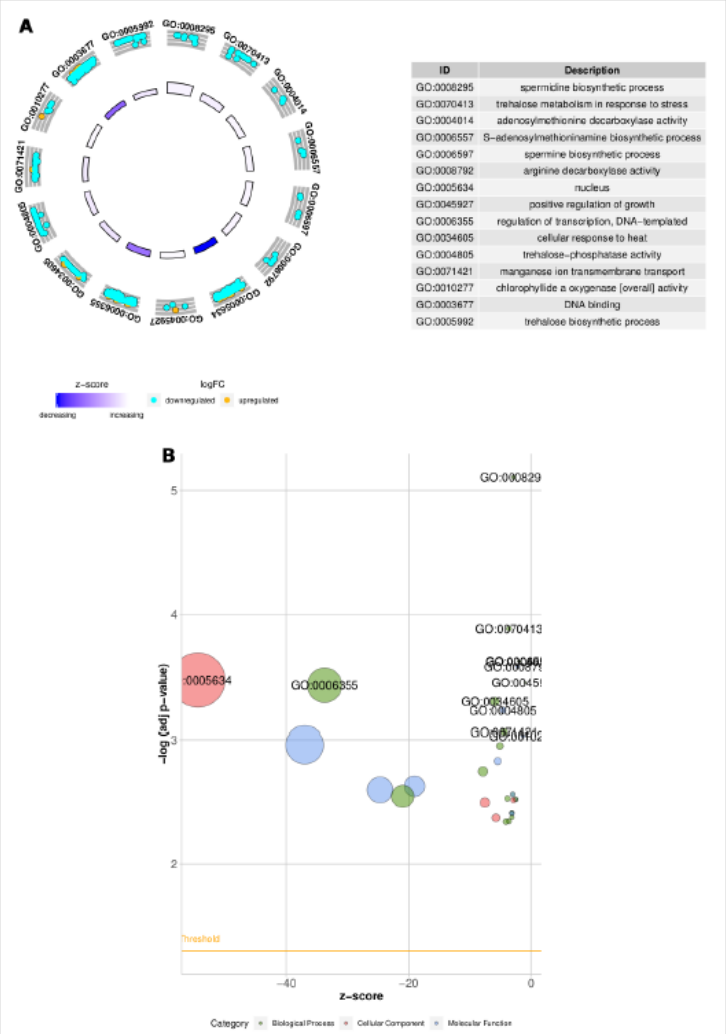

Figure 6

Functional differences in "Hoja de malvón" symptomatic vs. asymptomatic Vitis vinifera cv. Malbec plants. (A) Gene ontology terms with significant enrichment (p-value< 0,001) are represented as colored blocks in the inner ring based on z-score (numbers of upregulated genes minus number of downregulated genes grouped in each GO category) The differentially expressed genes in each category are represented as dots and colored based on LogFC values (cyan for downregulated and gold for upregulated). (B) Gene ontology terms represented according to its p-value significance in the hypergeometric test and z-score. The size of the circle represents the counts of genes in each GOterm category.

Supplementary Files

This is a list of supplementary files associated with this preprint. Click to download.

- TableS1.xlsx
- FigureS1.html
- TableS6.xlsx
- FigureS3.html
- TableS5.xlsx
- TableS3.xlsx
- FigureS4.html
- TableS4.xlsx
- FigureS2.html
- FigureS6.pdf
- FigureS5.pdf
- FigureS7.pdf